IEEE Access
Multidisciplinary ⋮ Rapid Review ⋮ Open Access Journal

Received 1 December 2023, accepted 22 December 2023, date of publication 8 January 2024, date of current version 3 May 2024.

Digital Object Identifier 10.1109/ACCESS.2024.3350734

RESEARCH ARTICLE

Simplified H1 Coil With a Single Layer of Surface Conductors

MAX KOEHLER[1] AND STEFAN M. GOETZ[2], (Member, IEEE)
[1]Department of Electrical and Computer Engineering, University of Kaiserslautern-Landau, 67663 Kaiserslautern, Germany
[2]Department of Psychiatry and Behavioral Sciences, Duke University, Durham, NC 27710, USA

Corresponding author: Max Koehler (m_koehle@rptu.de)

ABSTRACT Transcranial magnetic stimulation (TMS) is a popular method for the non-invasive stimulation of neurons in the human brain. It has become a standard instrument in experimental brain research and approved for a range of diagnostic and therapeutic applications in neurology and psychiatry. For major depressive disorder, TMS offers effective treatment with lower side effects than other therapies. Depression treatment is currently either performed with focal figure-of-eight coils or with rather distributed H1-type coils. In conventional protocols, the latter appears to even show superior performance. Still, their use is rather limited due to the complexity of the H coil. The H coil furthermore includes various segments that complicate manufacturing and drive the cost. In this paper, we present an electromagnetic equivalent for the H1 coil, which we call surface-projected, H1sp, through vector projection and Huygens' and Love's equivalence principle. The latter in principle allows to generate the electromagnetic field distribution inside a closed equivalence volume, e.g., a sphere, exclusively with currents on any closed surface around the volume. We aim at an anatomy-independent equivalent, i.e., the coil should generate the same induced electric field conditions as the original coil for any anatomy inside this equivalence volume, which matching in even a high number of sample anatomies could not fulfill. As the highest current utilization and efficiencies are achieved when all coil winding elements are as close to the target—i.e., the brain—as possible, we derived an equivalent entirely residing on a spherical shell on top of the head. In contrast to other coil design or optimization approaches, the procedure does not require any ad-hoc steps or heuristics but is an explicit forward Hilbert-space vector projection or base change. The resulting equivalent coil generates by design the same field conditions for any head anatomy inside but omits many complexity-, loss-, and leakage-flux-generating features of the initial H1 coil, such as the vertical coil winding segments or hard-to-manufacture sharp turns. For the same induced electric field magnitude and spatial profile, the equivalent H coil requires $<65\%$ of the magnetic field energy and $<55\%$ of the wire length. The comparably simple winding pattern promises the use of notable thicker wire than the initial H1 coil design with several relatively sharp corners.

INDEX TERMS Neuroscience, transcranial magnetic stimulation (TMS), coil design, coil equivalencies, H coil, treatment of major depression.

I. INTRODUCTION

Magnetic stimulation uses strong brief magnetic pulses to induce currents into the neural tissue and activate nerves [1], [2], [3], [4], [5]. Its transcranial form called TMS allows writing artificial signals into neurons and neural circuits inside the brain across the skull [6], [7]. Certain pulse rhythms and patterns can modulate neuronal circuits, i.e., influence how circuits process endogenous signals they receive [8]. TMS has become a key tool in experimental brain research and is widely used in medical diagnosis and treatment [9], [10], [11], [12]. It is, for example, cleared in various countries for the treatment of depression, bipolar disorder, obsessive compulsive disorder, smoking addiction, and migraine as well as for various diagnostic procedures and cortical mapping [13], [14], [15], [16], [17], [18], [19], [20], [21], [22], [23], [24], [25], [26]. TMS is also under investigation for many other disorders [6], [9], [27], [28], [29].

The associate editor coordinating the review of this manuscript and approving it for publication was Zhe Zhang.

The spatial distribution of the induced electric field determines which brain circuits are activated. The spatial field distribution is already substantially determined during the coil design phase where the shape of the conductors in the stimulation coil is set and positioning of the coil during stimulation [30]. Device manufacturers and researchers have developed a variety of different coils for TMS [31].

For clinical depression, TMS demonstrated effective treatment with fewer side effects as associated with convulsive interventions and many forms of medication, such as apathy and memory loss [14], [32], [33], [34], [35]. The approved procedures are twofold. Most prevalent is the focal stimulation in the dorsolateral prefrontal cortex with figure-of-eight coils [14], [15], [16], [17]. Figure-of-eight coils are practically part of every TMS device and therefore readily available. However, such focal stimulation requires good knowledge of the target and sophisticated technology [36]. Routine clinical settings, which often use rudimentary targeting, likely suffer from large position variability, resulting in low efficacy [37], [38].

The alternative procedure uses a comparably distributed stimulation pattern generated by the so-called H1 coil [13], [15], [17]. Potentially because of larger tolerance to inaccurate placement, maybe also due to the specific co-activation of various targets associated with the wider spread of the field, the treatment protocol used in conjuncture with the H coil demonstrated considerably higher remission rates ($\sim$33%) and response rates ($>$38%) compared to the figure-of-eight coil ($\sim$20% remission, $\sim$28% responders) in the double-blinded studies underlying the initial approval [13], [14]. Novel pulse patterns might enable reduced treatment durations [16], [39].

Despite the presumably superior efficacy according to the approval studies, the H coil is notably less frequently used for depression treatment than figure-of-eight coils. Furthermore, there is also substantially less research on improving it, e.g., with accelerated protocols. The reasons for the less frequent application are not of medical nature but mostly technical and logistical. The dominant reasons include the limited availability of H coils. Figure-of-eight coils, on the other hand, are standard equipment of practically every TMS set. The limited availability of H coils seems closely linked to the notably higher technical effort to manufacture these coils due to an involved complicated winding, further increasing manufacturing cost. Figure-of-eight coils, however, are comparably simple.

Moreover, the winding contains segments that are far from the head or even pointing away from the head surface, resulting in high pulse energies for sufficient stimulation strength, additional ohmic loss, and heating. Several relatively sharp edges and similar small features in the winding also require the use of wire with sufficient bending flexibility and therefore small enough cross section. Although many of those winding features might not reach into the brain due to the spatially low-pass-filtering influence of the coil–brain distance and be smaller than the manufacturing tolerance of the coils, the low cross section impacts the performance as it further increases heating. The heating in turn entails the need for a more powerful and therefore typically active cooling system. The consequence is a further increase in manufacturing complexity and cost.

There have been previous attempts to simplify historically complicated coils but many of such attempts have been widely ad-hoc, contain heuristic steps, or are fully manual. As the H coil was approved with the intricate winding features, however, any change would have to be substantially equivalent. Thus, the coil should generate the same induced electric field distribution with a deviation maybe only on the order of the manufacturing tolerance of the H1 coil to allow comparable activation patterns and maintain the regulatory clearance [40]. Accordingly, such a simplification of a coil winding should ideally not happen through manual trial and error. Instead, a transformation or projection guaranteeing mathematical and physical equivalence would be preferable. Previous research has optimized coils, which could in principle also serve for deriving equivalent coils [41], [42], [43], [52]. However, the use of a global optimization framework, typically including search heuristics, does not necessary guarantee equivalence and further appears computationally excessive if instead a forward projection transformation were possible, which is comparatively resource-efficient.

This article derives a notably simplified version of the H1 coil through projection, which we call H1sp for surface projection. The coil winding resides on a spherical surface with small distance to the head and eliminates coil elements pointing radially outwards as they can—following Huygens' and Love's principle and Maxwell's equations—not contribute to the magnetic or induced electric field inside. The simplifications reduce the field energy outside the head and also the winding resistance, while the coil winding features are simplified to allow for thicker wires with lower bending flexibility.

II. MATCHING PROCEDURE

This article aims at simplifying the H1 coil used for the treatment of major depression by finding an equivalent fully residing on a shell with 110 mm radius around the head through projection operation only. This radius ensures that the coil is applicable to a large part of the population while still not leaving large gaps between coil and head, which cost field energy; larger or smaller radiuses can be generated with the same formalism. The derived coil should generate an equivalent induced electric field profile as the H1 coil for any patient.

Since the coil should generate a practically equivalent induced electric field profile to the original H1 coil in any patient, i.e., any conceivable head and brain anatomy, we used a precursor of the induced electric field for matching. Matching based on the resulting induced electric field would require an entire ensemble of realistic head anatomies covering the full bandwidth of possible anatomic variability including of abnormalities to allow for a sufficiently tolerant

equivalency. As both the original H1 coil and the surface-projected H1 would generate the same anatomy-independent electromagnetic precursor of the electric field as suggested here, both would generate also the same electromagnetic (i.e., induced electric field) and physiological outcomes for any head anatomy as the same input to the Maxwell equations and all physiology enforces the same outcome.

The chosen matched physical quantity is the magnetic vector potential $\mathbf{A}$ inside the spherical shell, which fully determines the magnetic flux density $\mathbf{B}$ inside the shell through $\mathbf{B}(\mathbf{r}) = \mathbf{curl}\mathbf{A}(\mathbf{r}) = \nabla \times \mathbf{A}(\mathbf{r})$ at the location $\mathbf{r}$ with the **curl** operator curl [44]. With sufficiently equal magnetic vector potential $\mathbf{A}$ and magnetic flux density $\mathbf{B}$ inside the sphere, the induced electric field $\mathbf{E}$ inside will likewise match the original coil, no matter which anatomy or object is inside the volume.

The induced electric field can be derived through Faraday's law of induction, which reads $\mathbf{E}(\mathbf{r}) = -\frac{\partial}{\partial t}\mathbf{A}(\mathbf{r}) - \mathbf{grad}\phi(\mathbf{r})$ for the vector potential and the electrical potential distribution $\phi(\mathbf{r})$ in the vector analysis formalism [45], [46]. The first summand is often called the primary electric field, the second one the secondary electric field. The electrical potential underlying the secondary electric field is generated by the currents flowing in response to the induced currents, which accumulate at conductivity changes, e.g., at tissue interfaces or durae.

As a general solution space for all possible resulting coils, we define current distributions on a shell encompassing the head. To describe practically any possible coil residing on the surface, we use a continuous vector-valued current distribution $\mathbf{j}(\mathbf{r})$ at position $\mathbf{r}$. Its current distribution can also be represented by a sum of currents. If the solution space is designed as a complete infinite vector space, it can be given a vector base, and every possible solution can be represented as a sum of base vectors $\mathbf{b}_\mathrm{i}(\mathbf{r})$ each scaled appropriately by γ_i following $\mathbf{j}(\mathbf{r}) = \sum_\mathrm{i} \gamma_i \mathbf{b}_i(\mathbf{r})$. Without loss of generality, we used the harmonics on the spherical surface to form an orthonormal and complete basis in the coil current space.

The problem of finding the H1 coil match therefore becomes the finding for weights or coordinates γ_i. In contrast to any previous coil optimization approaches that use iterative search we defined a forward projection operation. We isomorphically matched the basis $\mathbf{b}_i$ of the coil current space with a corresponding basis $\mathbf{a}_i$ in the space of magnetic vector potentials according to $\mathbf{a}_i = \mathfrak{A}\{\mathbf{b}_i\}$, where the functional $\mathfrak{A}$ calculates the magnetic vector potential of the current distribution in its argument. Due to the linearity of $\mathfrak{A}$, $\mathfrak{A}\left(\sum_\mathrm{i} \gamma_i \mathbf{b}_i\right) = \sum_\mathrm{i} \gamma_i \mathfrak{A}(\mathbf{b}_i)$. We calculated the magnetic vector potential through Biot–Savart following the literature [45], [47]. We furthermore defined a bilinear inner product as $\langle \mathbf{A}_i, \mathbf{A}_j \rangle := \int \mathbf{A}_i(\mathbf{r})\,\mathbf{A}_j(\mathbf{r})\,\mathrm{d}^3 r$ for any vectors $\mathbf{A}_i$ for the necessary projection of a magnetic vector potential on the basis vectors and projected the magnetic vector potential $\mathbf{A}_{\mathrm{H1}}(\mathbf{r})$ of the H1 coil inside the region of interest VRIO onto the magnetic vector potentials of each coil current base vector $\mathbf{a}_i(\mathrm{r}) = \mathfrak{A}(\mathbf{b}_i)$ up to order $\mathrm{n} = 14$ here with the above-defined inner product per $\gamma_i = \langle \mathbf{A}_{\mathrm{H1}}(\mathbf{r}), \mathbf{a}_i(\mathbf{r}) \rangle = \int_{V_{RIO}} \mathbf{A}_{\mathrm{H1}}(\mathbf{r})\,\mathfrak{A}(\mathbf{b}_i)\,\mathrm{d}^3 r$. The spherical region of interest had a radius of 85 mm, approximately representing the dimensions human head. Spherical representations with those dimensions are well established in TMS [48], [49]. Importantly, the approach does not assume any spherical anatomy or similar simplification as used in the past, nor one or many real example anatomies but only uses the magnetic vector potential and thus the primary electric field for matching. The sphere restricts only the region of interest within which the same field conditions are generated and which should be larger than any expected head anatomy but stays naïve with respect to a specific anatomy. As the coil current space is designed isomorphic to the space of corresponding vector potentials, applying the resulting weighting coefficients results in the equivalent current distribution $\mathrm{j}_{\mathrm{equiv}}(\mathrm{r})$.

III. DISCRETIZATION OF THE EQUIVALENT SURFACE CURRENT DISTRIBUTION INTO COIL WIRE

We subsequently discretized the equivalent coil current distribution $\mathrm{j}_{\mathrm{equiv}}$ into specific wire turns a coil. In contrast to previous work that discretized continuous currents for a coil typically generated multiple unconnected closed loops first and then manually linked them more or less abruptly, we generate continuous wire representations along integral curves through a vector field which we generate from combining above $\mathrm{j}_{\mathrm{equiv}}$ with an auto-generated weighted gradient field $\mathbf{j}_{\mathrm{grad}}(\mathbf{r}) = \hat{\mathbf{n}}(\mathbf{r}) \times \mathbf{j}_{\mathrm{equiv}}(\mathbf{r})$, where $\hat{\mathbf{n}}$ is the normal vector of the surface in the point $\mathbf{r}$, which introduces the outward spiral. Combination of these two fields results in $\mathbf{j}_{\mathrm{res}}(\mathbf{r}) = \mathbf{j}_{\mathrm{equiv}}(\mathbf{r}) + k \cdot \frac{\mathbf{j}_{\mathrm{grad}}(\mathbf{r})}{\|\mathbf{j}_{\mathrm{grad}}(\mathbf{r})\|_2}$, where the weighting coefficient k controls the number of turns and thus the inductance.

Validation simulations in realistic head models were performed in SimNIBS v3.2.6 with the Ernie reference model.

IV. IMPLEMENTATION OF THE EQUIVALENT H1 COIL

We derived equivalent H1sp coils with various numbers of turns, representing different inductivities (Fig. 1). Out of these, we implemented a variant the factor k of 0.05 but enhanced the conductor length do form 12 turns, resulting in 16 μH to be in the upper range of typical TMS coils for moderately high currents in a prototype (Fig. 3). We transferred the winding pattern to a spherical polymer support and wound the coil with 5.4 m of 4 mm^2 magnet wire. The coil winding was connected to two 10 AWG braided cables (Alpha Wire 391045, Elizabeth (NJ), USA), resulting in a diameter of 10.5 mm^2, and an Anderson connector (Anderson Power SB-350, Ideal Industries, Sycamore (IL), USA). The coil with cable and connector was measured at 17.4 μH (Hameg Instruments HM8118, Frankfurt, Germany).

We sampled the induced electric field of the H1sp prototype under spherical constraints using an automated field probe as described in more detail in the literature [49]. The coil was connected to a commercial MagVenture MagLite pulse source (Tonica, Farum Denmark) with biphasic pulses (standard mode).

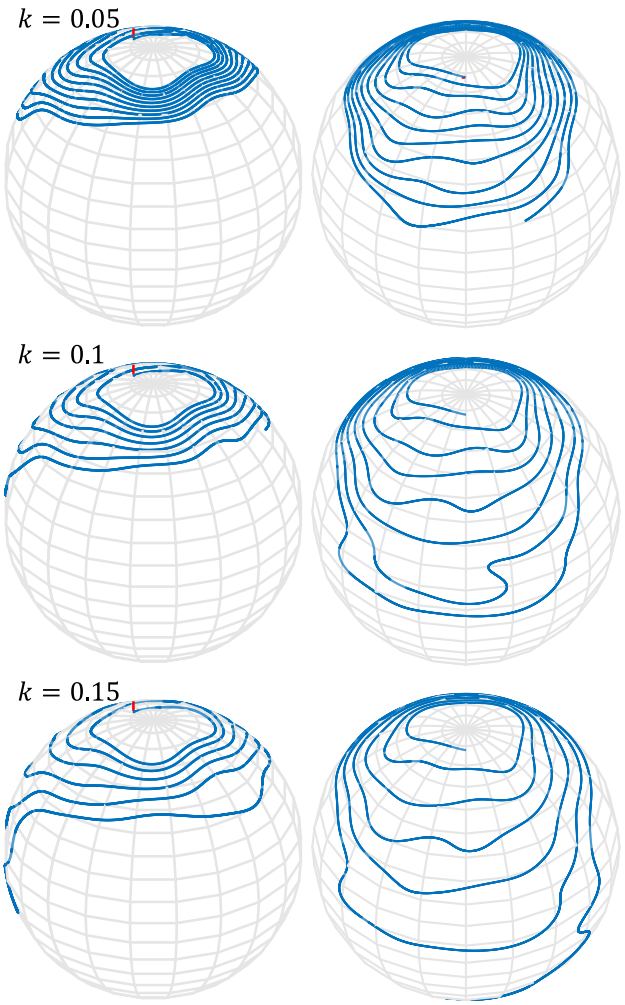

FIGURE 1. Three equivalent quantizations of the H1 coil on a spherical surface (left: front view, right: back view) with different k factors 0.05 (10.36 μH), 0.1 (5.79 μH), and 0.15 (3.93 μH).

V. PROJECTION RESULTS

The equivalent mapping process leads to an H1sp coil embodiment with relative primary field error

$$\delta = \frac{1}{2E_{\text{prim,H1orig,max}}} \times \int_{V_{\text{ROI}}} \left\| \mathbf{E}_{\text{prim,H1orig}}(\mathbf{r}) - \mathbf{E}_{\text{prim,H1sp}}(\mathbf{r}) \right\|_2 \mathrm{d}^3 r$$

of 8.4%.

Figure 1 displays three discretized H1sp coils with different numbers of turns. The coils feature a high winding density in the frontal area at the same point where the original H1 coil, H1orig, has the highest winding density, leading to a strong induced electric field underneath. The H1orig coil does not have any windings posterior as the turns lift off the head not too far from the central gyrus and connect to a junction box. The winding and the current have to be closed, and the equivalent H1sp intentionally does not want to lift the winding but keep it on the spherical surface to avoid leakage flux that does not interact with the brain but unnecessarily increases the field energy and the resistance. Therefore, the mapping spreads the windings out in the posterior part, effectively reducing the induced electric field there. In contrast to the H1orig coil, the H1sp does not have any sharp edges, suggesting that those features would not be induced into the brain anyway due to the smoothening effect of the coil–brain distance.

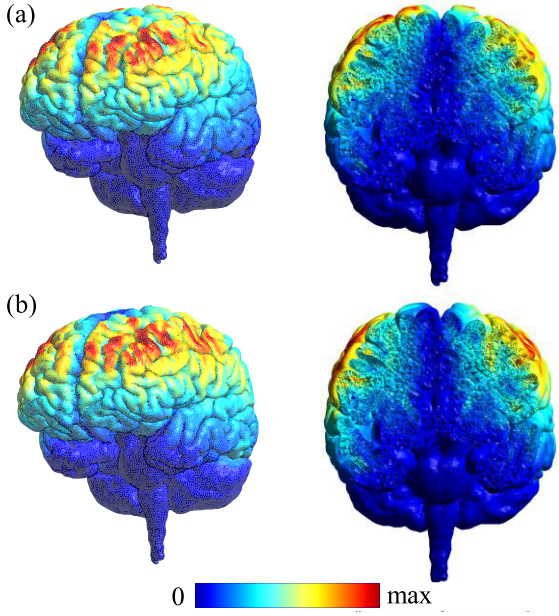

FIGURE 2. Electric field distributions of (a) the original H1 and (b) the equivalent H1sp coil simulated in a realistic head to demonstrate the field fingerprint in the dorsolateral prefrontal cortex and the depth in the sagittal section. The color coding is standardized to the same amplitude in both (a) and (b), where the maximum value would correspond to an electric field amplitude of 50 V/m at 20 A/μs (e.g., 1700 A for 3 kHz) here.

The frontal winding part still has a long almost straight transverse section, reflecting the corresponding parts of the H1orig coil. The H1orig coil, however, needs two overlapping sets of windings to generate the same frontal field pattern, which the H1sp coil projected onto the simple resulting shape. The overall H1sp shape is not fully symmetric between the left and the right side, which reflects the subtle asymmetry of the H1orig coil, where a large share of the windings lifts off the head approximately one inch more anterior than on the left side [50]. This asymmetry seems justified considering the primary treatment focus on the left dorsolateral prefrontal cortex (DLPFC). In the spherical H1sp coil, this asymmetry leads to a somewhat trapezoidal character of the innermost turns.

Figure 2 displays the induced electric fields of the original H1 coil and the spherically projected H1sp side-by-side in one specific head anatomy. Since the magnetic vector potential and therefore the primary and—for the same anatomies as well as coil positions—also the secondary electric fields are matched by design in general anatomies, the induced electric field in the realistic head models in Fig. 2 demonstrate comparable distribution and spread in depth as expected. For both, the dominant field is in the prefrontal cortex, whereas

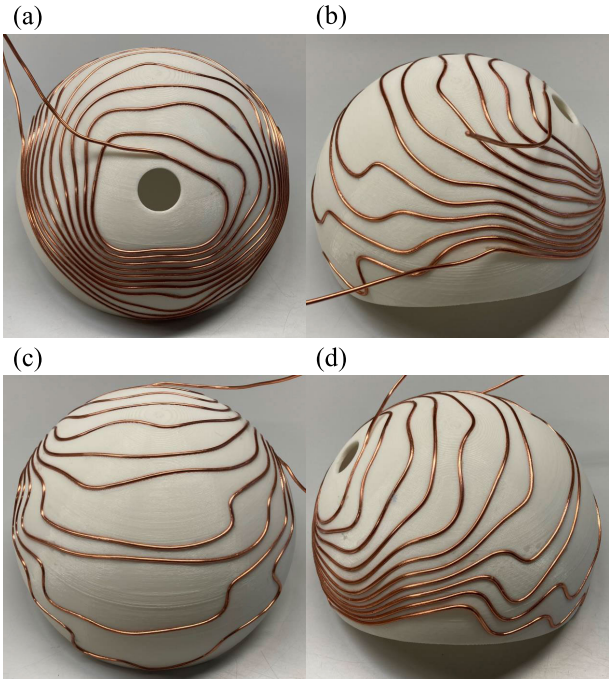

FIGURE 3. Implemented demonstrator of the equivalent H1 coil from various perspectives: (a) front, (b) right, (c) back, and (d) left.

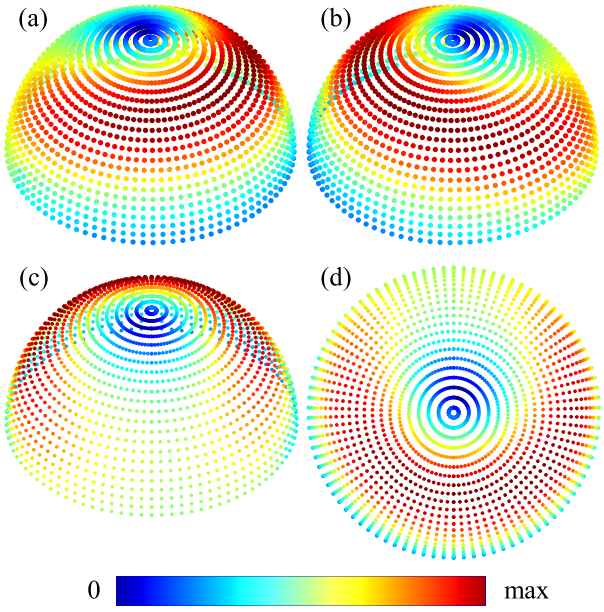

FIGURE 4. Measured electric field distribution of the prototype of Figure 3: (a) front-right, (b) front-left, (c) back and (d) top.

the field drops similarly slowly with half of the maximum field strength reached at a bit more than 2 cm below the cortex. The substantially deeper penetration of the electric field than figure-of-eight coils is a well-known feature of the H1 coil and may contribute to its high treatment efficacy [51].

The practical implementation of the H1sp on the shell (see Fig. 3) was simple compared to the original H1 with its two sets of overlapping windings, which need good insulation coordination in between, sharp features, and a terminal block, which drive the manufacturing cost. Matched to generate equivalent field strength for the same current, the coil has only approximately 52% of the length of the wire of an original H1 coil, which would allow reducing the heating by 48% for the same wire cross section and same induced electric field. The reduction in inductance and thus also the magnetic field energy amounts to 37.5%. Although, systematic projection and optimization methods may be new, the electromagnetics of coils is well understood, and models known to be highly accurate [53], [54], [55], [56], [57], [58], [59], [60]. Accordingly, the measured field (Fig. 4) does not entail surprises but reflects the simulations with a strong frontal component and little posterior field, features that have been discovered and promoted previously for the original H1 coil.

VI. CONCLUSION

This article derived a simpler equivalent of the H1 coil used primarily for the treatment of major depressive disorder on a (spherical) surface closely encompassing the head. The equivalency was generated by design using Huygens' and Love's principle that a field distribution inside a volume can be generated also by a current distribution on a shell around this volume so that no overlapping or vertical winding elements as used in the original H1 coil are physically necessary. The magnetic vector potential of the original H1 coil was mapped onto surface currents out of which a new coil with discrete windings could be generated.

In contrast to any previous coil optimization or design approaches, we used an explicit forward procedure without any iterations, optimization, or heuristic elements and can generate very simple projected H1 coils with practically any inductance. The H1sp coil has a simpler winding with only one continuous wire path without any overlaps or vertical elements, which promises to substantially streamline manufacturing of H1 coils in the future. These constraints on the winding pattern, primarily the non-overlapping of the conductors on a predefined surface, enable winding on a prefabricated polymer former which, firstly, can nowadays be produced cost-effectively using additive manufacturing methods as well as plastic molding and, secondly, greatly simplifies the winding process while drastically increasing accuracy and reproducibility With less than half the coil heating, a reduction of the enormous cooling system needed in previous H1 coils appears obvious and promises further cost reductions for manufacturers and ideally also users.

AVAILABILITY

The coil specifications and design data are available upon request.

ACKNOWLEDGMENT

The authors are inventors on patents and patent applicants for brain stimulation technology including coil technology and features used in this article held by current and previous employers.

REFERENCES

[1] M. J. R. Polson, A. T. Barker, and I. L. Freeston, "Stimulation of nerve trunks with time-varying magnetic fields," *Med. Biol. Eng. Comput.*, vol. 20, no. 2, pp. 243–244, Mar. 1982.

[2] Y. Ugawa, J. C. Rothwell, B. L. Day, P. D. Thompson, and C. D. Marsden, "Magnetic stimulation over the spinal enlargements," *J. Neurol., Neurosurg. Psychiatry*, vol. 52, no. 9, pp. 1025–1032, Sep. 1989.

[3] R. Nardone, Y. Höller, A. Taylor, A. Thomschewski, A. Orioli, V. Frey, E. Trinka, and F. Brigo, "Noninvasive spinal cord stimulation: Technical aspects and therapeutic applications," *Neuromodulation, Technol. Neural Interface*, vol. 18, no. 7, pp. 580–591, Oct. 2015.

[4] J. Szecsi, S. Götz, W. Pöllmann, and A. Straube, "Force–pain relationship in functional magnetic and electrical stimulation of subjects with paresis and preserved sensation," *Clin. Neurophysiol.*, vol. 121, no. 9, pp. 1589–1597, Sep. 2010.

[5] S. M. Goetz, H.-G. Herzog, N. Gattinger, and B. Gleich, "Comparison of coil designs for peripheral magnetic muscle stimulation," *J. Neural Eng.*, vol. 8, no. 5, Oct. 2011, Art. no. 056007.

[6] P. M. Rossini et al., "Non-invasive electrical and magnetic stimulation of the brain, spinal cord, roots and peripheral nerves: Basic principles and procedures for routine clinical and research application. An updated report from an I.F.C.N. committee," *Clin. Neurophysiol.*, vol. 126, no. 6, pp. 1071–1107, Jun. 2015.

[7] A. T. Barker, R. Jalinous, and I. L. Freeston, "Non-invasive magnetic stimulation of human motor cortex," *Lancet*, vol. 325, no. 8437, pp. 1106–1107, May 1985.

[8] A. Valero-Cabré, J. L. Amengual, C. Stengel, A. Pascual-Leone, and O. A. Coubard, "Transcranial magnetic stimulation in basic and clinical neuroscience: A comprehensive review of fundamental principles and novel insights," *Neurosci. Biobehav. Rev.*, vol. 83, pp. 381–404, Dec. 2017.

[9] S. Luan, I. Williams, K. Nikolic, and T. G. Constandinou, "Neuromodulation: Present and emerging methods," *Frontiers Neuroeng.*, vol. 7, Jul. 2014.

[10] A. T. Sack, R. Cohen Kadosh, T. Schuhmann, M. Moerel, V. Walsh, and R. Goebel, "Optimizing functional accuracy of TMS in cognitive studies: A comparison of methods," *J. Cognit. Neurosci.*, vol. 21, no. 2, pp. 207–221, Feb. 2009.

[11] C. Miniussi, M. Ruzzoli, and V. Walsh, "The mechanism of transcranial magnetic stimulation in cognition," *Cortex*, vol. 46, no. 1, pp. 128–130, Jan. 2010.

[12] B. Luber and S. H. Lisanby, "Enhancement of human cognitive performance using transcranial magnetic stimulation (TMS)," *NeuroImage*, vol. 85, pp. 961–970, Jan. 2014.

[13] Y. Levkovitz et al., "Efficacy and safety of deep transcranial magnetic stimulation for major depression: A prospective multicenter randomized controlled trial," *World Psychiatry*, vol. 14, no. 1, pp. 64–73, Feb. 2015.

[14] J. C. Ballenger, "Efficacy and safety of transcranial magnetic stimulation in the acute treatment of major depression: A multisite randomized controlled trial," *Yearbook Psychiatry Appl. Mental Health*, vol. 2009, pp. 219–220, Jan. 2009.

[15] M. S. George, S. H. Lisanby, D. Avery, W. M. McDonald, V. Durkalski, and M. Pavlicova, "Daily left prefrontal transcranial magnetic stimulation therapy for major depressive disorder: A sham-controlled randomized trialmagnetic stimulation for major depressive disorder," *Arch. Gen. Psychiatry*, vol. 67, pp. 507–516, Jan. 2010.

[16] D. M. Blumberger, F. Vila-Rodriguez, K. E. Thorpe, K. Feffer, Y. Noda, P. Giacobbe, Y. Knyahnytska, S. H. Kennedy, R. W. Lam, Z. J. Daskalakis, and J. Downar, "Effectiveness of theta burst versus high-frequency repetitive transcranial magnetic stimulation in patients with depression (THREE-D): A randomised non-inferiority trial," *Lancet*, vol. 391, no. 10131, pp. 1683–1692, Apr. 2018.

[17] Food and Drug Administration. (2013). *K122288; 510(K) Summary Brainsway Deep TMS System.* [Online]. Available: http://www.accessdata.fda.gov/cdrh_docs/pdf12/K122288.pdf

[18] A. Mantovani, H. B. Simpson, B. A. Fallon, S. Rossi, and S. H. Lisanby, "Randomized sham-controlled trial of repetitive transcranial magnetic stimulation in treatment-resistant obsessive-compulsive disorder," *Int. J. Neuropsychopharmacol.*, vol. 13, pp. 217–227, Jan. 2010.

[19] R. B. Lipton, D. W. Dodick, S. D. Silberstein, J. R. Saper, S. K. Aurora, S. H. Pearlman, R. E. Fischell, P. L. Ruppel, and P. J. Goadsby, "Single-pulse transcranial magnetic stimulation for acute treatment of migraine with aura: A randomised, double-blind, parallel-group, sham-controlled trial," *Lancet Neurol.*, vol. 9, no. 4, pp. 373–380, Apr. 2010.

[20] T. Picht, S. Schmidt, S. Brandt, D. Frey, H. Hannula, T. Neuvonen, J. Karhu, P. Vajkoczy, and O. Suess, "Preoperative functional mapping for rolandic brain tumor surgery: Comparison of navigated transcranial magnetic stimulation to direct cortical stimulation," *Neurosurgery*, vol. 69, no. 3, pp. 581–589, 2011.

[21] S. Takahashi and T. Picht, "Comparison of navigated transcranial magnetic stimulation to direct electrical stimulation for mapping the motor cortex prior to brain tumor resection," in *Tumors of the Central Nervous System*, vol. 12, M. A. Hayat, Ed. Dordrecht, The Netherlands: Springer, 2014, pp. 261–276.

[22] A. Zangen, H. Moshe, D. Martinez, N. Barnea-Ygael, T. Vapnik, and A. Bystritsky, "Repetitive transcranial magnetic stimulation for smoking cessation: A pivotal multicenter double-blind randomized controlled trial," *World Psychiatry*, vol. 20, pp. 397–404, 2021.

[23] *Transcranial Magnetic Stimulation for Treating and Preventing Migraine*, U.K. National Institute for Health and Cade Excellence (NICE), London, U.K., 2014.

[24] U.K. National Institute for Health and Cade Excellence (NICE). (2007). *Transcranial Magnetic Stimulation for Severe Depression*. [Online]. Available: https://www.nice.org.uk/Guidance/ipg242

[25] U.K. National Institute for Health and Cade Excellence (NICE). (2015). *Repetitive Transcranial Magnetic Stimulation for Depression*. NICE Interventional Procedure Guidance IPG542. [Online]. Available: https://www.nice.org.uk/guidance/ipg542

[26] J. Mutz, D. R. Edgcumbe, A. R. Brunoni, and C. H. Y. Fu, "Efficacy and acceptability of non-invasive brain stimulation for the treatment of adult unipolar and bipolar depression: A systematic review and meta-analysis of randomised sham-controlled trials," *Neurosci. Biobehav. Rev.*, vol. 92, pp. 291–303, Sep. 2018.

[27] M. C. Eldaief, D. Z. Press, and A. Pascual-Leone, "Transcranial magnetic stimulation in neurology: A review of established and prospective applications," *Neurol. Clin. Pract.*, vol. 3, no. 6, pp. 519–526, Dec. 2013.

[28] T. Marzouk, S. Winkelbeiner, H. Azizi, A. K. Malhotra, and P. Homan, "Transcranial magnetic stimulation for positive symptoms in schizophrenia: A systematic review," *Neuropsychobiology*, vol. 79, no. 6, pp. 384–396, 2020.

[29] F. Fisicaro, G. Lanza, A. A. Grasso, G. Pennisi, R. Bella, W. Paulus, and M. Pennisi, "Repetitive transcranial magnetic stimulation in stroke rehabilitation: Review of the current evidence and pitfalls," *Therapeutic Adv. Neurolog. Disorders*, vol. 12, Jan. 2019, Art. no. 175628641987831.

[30] S. M. Goetz and Z.-D. Deng, "The development and modelling of devices and paradigms for transcranial magnetic stimulation," *Int. Rev. Psychiatry*, vol. 29, no. 2, pp. 115–145, Mar. 2017.

[31] A. V. Peterchev, Z. D. Deng, and S. M. Goetz, "Advances in transcranial magnetic stimulation technology," in *Brain Stimulation*. Hoboken, NJ, USA: Wiley, 2015, pp. 165–189.

[32] G. Serafini, M. Pompili, M. B. Murri, M. Respino, L. Ghio, P. Girardi, P. B. Fitzgerald, and M. Amore, "The effects of repetitive transcranial magnetic stimulation on cognitive performance in treatment-resistant depression. A systematic review," *Neuropsychobiology*, vol. 71, no. 3, pp. 125–139, 2015.

[33] J. Prudic, "Strategies to minimize cognitive side effects with ECT: Aspects of ECT technique," *J. ECT*, vol. 24, no. 1, pp. 46–51, 2008.

[34] V. Snow, S. Lascher, and C. Mottur-Pilson, "Pharmacologic treatment of acute major depression and dysthymia: Clinical guideline, Part 1," *Ann. Internal Med.*, vol. 132, no. 9, p. 738, May 2000.

[35] D. E. Kemp, "Managing the side effects associated with commonly used treatments for bipolar depression," *J. Affect. Disorders*, vol. 169, pp. S34–S44, Dec. 2014.

[36] S. M. Goetz and T. Kammer, "Neuronavigation," in *Oxford Handbook of Transcranial Stimulation*, E.M. Wassermann, C. M. Epstein, A. V. Peterchev, U. Ziemann, V. Walsh, and T. Paus, Eds. Oxford, U.K.: Oxford Univ. Press, 2020.

[37] J.-P. Lefaucheur, "Why image-guided navigation becomes essential in the practice of transcranial magnetic stimulation," *Neurophysiologie Clinique/Clin. Neurophysiol.*, vol. 40, no. 1, pp. 1–5, Mar. 2010.

[38] M.-L. Paillère Martinot, A. Galinowski, D. Ringuenet, T. Gallarda, J.-P. Lefaucheur, F. Bellivier, C. Picq, P. Bruguière, J.-F. Mangin, D. Rivière, J.-C. Willer, B. Falissard, M. Leboyer, J.-P. Olié, E. Artiges, and J.-L. Martinot, "Influence of prefrontal target region on the efficacy of repetitive transcranial magnetic stimulation in patients with medication-resistant depression: A [18F]-fluorodeoxyglucose PET and MRI study," *Int. J. Neuropsychopharmacology*, vol. 13, no. 1, p. 45, Feb. 2010.

[39] Y.-Z. Huang, M. J. Edwards, E. Rounis, K. P. Bhatia, and J. C. Rothwell, "Theta burst stimulation of the human motor cortex," *Neuron*, vol. 45, no. 2, pp. 201–206, Jan. 2005.
[40] M. Tzirini, Y. Roth, T. Harmelech, S. Zibman, G. S. Pell, V. Kimiskidis, A. Tendler, A. Zangen, and T. Samaras, "Electrical field measurements and simulations of the H7 and D-B80 coils: Non-equivalence of the TMS coils for obsessive compulsive disorder," *Brain Stimulation*, vol. 14, no. 6, pp. 1525–1527, Nov. 2021.
[41] L. J. Gomez, S. M. Goetz, and A. V. Peterchev, "Design of transcranial magnetic stimulation coils with optimal trade-off between depth, focality, and energy," *J. Neural Eng.*, vol. 15, no. 4, Aug. 2018, Art. no. 046033.
[42] B. Wang, M. R. Shen, Z.-D. Deng, J. E. Smith, J. J. Tharayil, C. J. Gurrey, L. J. Gomez, and A. V. Peterchev, "Redesigning existing transcranial magnetic stimulation coils to reduce energy: Application to low field magnetic stimulation," *J. Neural Eng.*, vol. 15, no. 3, Jun. 2018, Art. no. 036022.
[43] L. M. Koponen, J. O. Nieminen, and R. J. Ilmoniemi, "Minimum-energy coils for transcranial magnetic stimulation: Application to focal stimulation," *Brain Stimulation*, vol. 8, no. 1, pp. 124–134, Jan. 2015.
[44] J. D. Jackson, *Classical Electrodynamics*. New York, NY, USA: Wiley, 2007.
[45] S. M. Goetz, J. Kammermann, F. Helling, T. Weyh, and Z. Li, "Force recruitment of neuromuscular magnetic stimulation predicted through high-resolution anatomical 3D models," *BioRxiv*, pp. 1–14, Dec. 2021, doi: 10.1101/2021.12.25.474143.
[46] S. M. Goetz, T. Weyh, I. A. A. Afinowi, and H.-G. Herzog, "Coil design for neuromuscular magnetic stimulation based on a detailed 3-D thigh model," *IEEE Trans. Magn.*, vol. 50, no. 6, pp. 1–10, Jun. 2014.
[47] S. M. Goetz, H.-G. Herzog, and T. Weyh, "A realistic model for approaching the activation question of neuromuscular magnetic stimulation," in *Proc. 6th Int. IEEE/EMBS Conf. Neural Eng. (NER)*, Nov. 2013, pp. 331–334.
[48] A. Nummenmaa, M. Stenroos, R. J. Ilmoniemi, Y. C. Okada, M. S. Hämäläinen, and T. Raij, "Comparison of spherical and realistically shaped boundary element head models for transcranial magnetic stimulation navigation," *Clin. Neurophysiol.*, vol. 124, no. 10, pp. 1995–2007, Oct. 2013.
[49] J. O. Nieminen, L. M. Koponen, and R. J. Ilmoniemi, "Experimental characterization of the electric field distribution induced by TMS devices," *Brain Stimulation*, vol. 8, no. 3, pp. 582–589, May 2015.
[50] Y. Roth, A. Amir, Y. Levkovitz, and A. Zangen, "Three-dimensional distribution of the electric field induced in the brain by transcranial magnetic stimulation using figure-8 and deep H-coils," *J. Clin. Neurophysiol.*, vol. 24, no. 1, pp. 31–38, 2007.
[51] S. Zibman, G. S. Pell, N. Barnea-Ygael, Y. Roth, and A. Zangen, "Application of transcranial magnetic stimulation for major depression: Coil design and neuroanatomical variability considerations," *Eur. Neuropsychopharmacology*, vol. 45, pp. 73–88, Apr. 2021.
[52] F. Tang, J. Hao, F. Freschi, C. Niu, M. Repetto, F. Liu, and S. Crozier, "A cone-shaped gradient coil design for high-resolution MRI head imaging," *Phys. Med. Biol.*, vol. 64, no. 8, Apr. 2019, Art. no. 085003.
[53] M. Chen and D. J. Mogul, "Using increased structural detail of the cortex to improve the accuracy of modeling the effects of transcranial magnetic stimulation on neocortical activation," *IEEE Trans. Biomed. Eng.*, vol. 57, no. 5, pp. 1216–1226, May 2010.
[54] M. Daneshzand, S. N. Makarov, L. I. N. de Lara, B. Guerin, J. McNab, B. R. Rosen, M. S. Hämäläinen, T. Raij, and A. Nummenmaa, "Rapid computation of TMS-induced E-fields using a dipole-based magnetic stimulation profile approach," *NeuroImage*, vol. 237, Aug. 2021, Art. no. 118097.
[55] L. Golestanirad, M. Mattes, J. R. Mosig, and C. Pollo, "Effect of model accuracy on the result of computed current densities in the simulation of transcranial magnetic stimulation," *IEEE Trans. Magn.*, vol. 46, no. 12, pp. 4046–4051, Dec. 2010.
[56] L. J. Gomez, M. Dannhauer, L. M. Koponen, and A. V. Peterchev, "Conditions for numerically accurate TMS electric field simulation," *Brain Stimulation*, vol. 13, no. 1, pp. 157–166, Jan. 2020.
[57] S. N. Makarov, G. M. Noetscher, E. H. Burnham, and D. N. Pham, "Software toolkit for fast high-resolution TMS modeling," *BioRxiv*, p. 643346, May 2019.
[58] S. N. Makarov, W. A. Wartman, G. M. Noetscher, K. Fujimoto, T. Zaidi, E. H. Burnham, M. Daneshzand, and A. Nummenmaa, "Degree of improving TMS focality through a geometrically stable solution of an inverse TMS problem," *NeuroImage*, vol. 241, Nov. 2021, Art. no. 118437.
[59] A. V. Mancino, F. E. Milano, F. M. Bertuzzi, C. G. Yampolsky, L. E. Ritacco, and M. R. Risk, "Obtaining accurate and calibrated coil models for transcranial magnetic stimulation using magnetic field measurements," *Med. Biol. Eng. Comput.*, vol. 58, no. 7, pp. 1499–1514, Jul. 2020.
[60] F. S. Salinas, J. L. Lancaster, and P. T. Fox, "3D modeling of the total electric field induced by transcranial magnetic stimulation using the boundary element method," *Phys. Med. Biol.*, vol. 54, no. 12, pp. 3631–3647, Jun. 2009.

MAX KOEHLER received the Dipl.-Ing. degree from Technische Universität Kaiserslautern, Kaiserslautern, Germany, in 2021. Since 2021, he has been a Research Assistant with the Chair of Mechatronics and Electrical Drives, University of Kaiserslautern-Landau. His current research interests include coil design and optimization for magnetic neurostimulation, noninvasive brain stimulation, and magnetic materials applied to transcranial magnetic stimulation.

STEFAN M. GOETZ (Member, IEEE) received the bachelor's and master's degrees from the Technical University of Munich (TU München), Munich, Germany, and the Ph.D. degree from TU München and Columbia University. His research interests include neuroelectronics, electromagnetic fields and their generation, high-performance electronics, neurophysiology, and scientific instrumentation.